

An $S = 2$ Cyanide-Bridged Trinuclear $\text{Fe}^{\text{III}}_2\text{Ni}^{\text{II}}$ Single-Molecule MagnetDongfeng Li,[†] Rodolphe Clérac,^{*‡} Sean Parkin,[†] Guangbin Wang,[§] Gordon T. Yee,[§] and Stephen M. Holmes^{*†}

Department of Chemistry, University of Kentucky, Lexington, Kentucky 40506-0055, Centre de Recherche Paul Pascal, UPR-CNRS 8641, 115 avenue du Dr. A. Schweitzer, 33600 Pessac, France, and Department of Chemistry, Virginia Polytechnic Institute and State University, Blacksburg, Virginia 24061

Received March 7, 2006

Treatment of $[\text{NEt}_4][(\text{pzTp})\text{Fe}^{\text{III}}(\text{CN})_3]$ (**1**) with $\text{Ni}^{\text{II}}(\text{OTf})_2$ ($\text{OTf} =$ trifluoromethanesulfonate) and 1,5,8,12-tetraazadodecane (**L**) affords $\{[(\text{pzTp})\text{Fe}^{\text{III}}(\text{CN})_3]_2[\text{Ni}^{\text{II}}(\text{L})]\} \cdot \frac{1}{2}\text{MeOH}$ (**2**), while 2,2'-bipyridine (**bipy**) affords $\{[(\text{pzTp})\text{Fe}^{\text{III}}(\text{CN})_3]_2[\text{Ni}^{\text{II}}(\text{bipy})_2]\} \cdot 2\text{H}_2\text{O}$ (**3**). Magnetic measurements indicate that **2** and **3** have $S = 2$ ground states and that **3** exhibits slow relaxation of the magnetization above 2 K.

The burgeoning field of single-molecule magnet (SMM) materials has seen extensive activity over the past decade. These inorganic complexes exhibit superparamagnetic-like behavior owing to the large spin ground state (S) and Ising-type anisotropy ($D < 0$ and small E) derived from the transition-metal centers used in their construction.¹ These characteristics create an energy barrier (Δ) between the two thermodynamically equivalent $m_S = \pm S$ configurations. Hence, below T_B , the so-called blocking temperature, the thermal energy is insufficient to overcome Δ and the spin is trapped in one of the two configurations. Application of large magnetic fields (H_{dc}) saturates the magnetization (M) of the sample, and removal of this field ($H_{\text{dc}} = 0$) will induce a slow decay of M toward zero with a characteristic relaxation time (τ). The relaxation time usually exhibits thermally activated behavior and can be measured using the time dependence of M or, more commonly, the frequency (ν) dependence of the ac susceptibility. At very low temperatures, quantum tunneling of the magnetization (QTM) often relaxes the magnetization at rates faster than thermally activated pathways. Experimentally, a crossover occurs between these two regimes, and in this intermediate temperature range, the thermal barrier (Δ) is circumvented by quantum tunneling, affording an effective barrier Δ_{eff} .¹

While the vast majority of SMMs are derived from metal centers linked by oxo and carboxylate ligands, several groups

have recently described that such complexes can also be prepared from $[\text{fac-L}^m\text{M}^n(\text{CN})_3]^{n+m-3}$ units.² The preparation of these cyanometalate complexes utilizes a building-block synthetic approach, where discrete molecular precursors are allowed to self-assemble into a common structural archetype, allowing for detailed structure–property relationships to be described. As part of a continuing effort to develop structurally related cyanometalate SMMs, we recently developed a series of poly(pyrazolylborate) cyanometalate building blocks and have systematically investigated the controlled aggregation of these units into complexes and networks.³ Herein, we report on the synthesis, structures, and spectroscopic and magnetic properties of two trinuclear $\text{Fe}^{\text{III}}_2\text{Ni}^{\text{II}}$ complexes, $\{[(\text{pzTp})\text{Fe}^{\text{III}}(\text{CN})_3]_2[\text{Ni}^{\text{II}}(\text{L})]\} \cdot \frac{1}{2}\text{MeOH}$ (**2**; **L** = 1,5,8,12-tetraazadodecane) and $\{[(\text{pzTp})\text{Fe}^{\text{III}}(\text{CN})_3]_2[\text{Ni}^{\text{II}}(\text{bipy})_2]\} \cdot 2\text{H}_2\text{O}$ (**3**; **bipy** = 2,2'-bipyridine), of which the latter exhibits slow relaxation of the magnetization above 2 K.

Treatment of $[\text{NEt}_4][(\text{pzTp})\text{Fe}^{\text{III}}(\text{CN})_3]$ (**1**) with nickel(II) trifluoromethanesulfonate and 1,5,8,12-tetraazadodecane (**L**) or 2,2'-bipyridine (**bipy**) in methanol cleanly affords red **2** and orange **3** as crystalline solids.^{3c,4,5} The infrared spectra exhibit intense ν_{CN} stretching absorptions at 2137 and 2122 cm^{-1} for **2** and at 2162 and 2119 cm^{-1} for **3** that are tentatively assigned as bridging and terminal cyanides, respectively.³

Compound **2** crystallizes in the triclinic $P\bar{1}$ space group.^{4,5} The neutral complex consists of a central octahedral $[\text{Ni}^{\text{II}}(\text{L})]^{2+}$ unit that is linked to two $[(\text{pzTp})\text{Fe}^{\text{III}}(\text{CN})_3]^-$ anions (Figure 1), via bridging cyanides, that are axial to the coordinated 1,5,8,12-tetraazadodecane ligand. The Ni–N bond distances for the *trans*-cyanides are 2.109(6) (Ni1–

* To whom correspondence should be addressed. E-mail: smholm2@uky.edu (S.M.H.), clerac@crpp-bordeaux.cnrs.fr (R.C.).

[†] University of Kentucky.

[‡] UPR-CNRS 8641.

[§] Virginia Polytechnic Institute and State University.

(1) (a) Sessoli, R.; Gatteschi, D. *Angew. Chem., Int. Ed.* **2003**, *42*, 268–297 and references cited therein. (b) Beltran, L. M. C.; Long, J. R. *Acc. Chem. Res.* **2005**, *38*, 325–334 and references cited therein.

(2) (a) Schelter, E. J.; Prosvirin, A. V.; Dunbar, K. R. *J. Am. Chem. Soc.* **2004**, *126*, 15004–15005. (b) Wang, S.; Zou, J.-L.; Zhou, H.-C.; Choi, H. J.; Ke, Y.; Long, J. R.; You, X.-Z. *Angew. Chem., Int. Ed.* **2004**, *43*, 5940–5943. (c) Sokol, J. J.; Hee, A. G.; Long, J. R. *J. Am. Chem. Soc.* **2002**, *124*, 7656–7657.

(3) (a) Li, D.; Parkin, S.; Wang, G.; Yee, G. T.; Prosvirin, A. V.; Holmes, S. M. *Inorg. Chem.* **2005**, *44*, 4903–4905. (b) Li, D.; Parkin, S.; Wang, G.; Yee, G. T.; Holmes, S. M. *Inorg. Chem.* **2006**, *45*, 1951–1959. (c) Li, D.; Parkin, S.; Wang, G.; Yee, G. T.; Clérac, R.; Wernsdorfer, W.; Holmes, S. M. *J. Am. Chem. Soc.* **2006**, *128*, 4212–4215. (d) Li, D.; Parkin, S.; Wang, G.; Yee, G. T.; Holmes, S. M. *Inorg. Chem.* **2006**, *45*, 2773–2775.

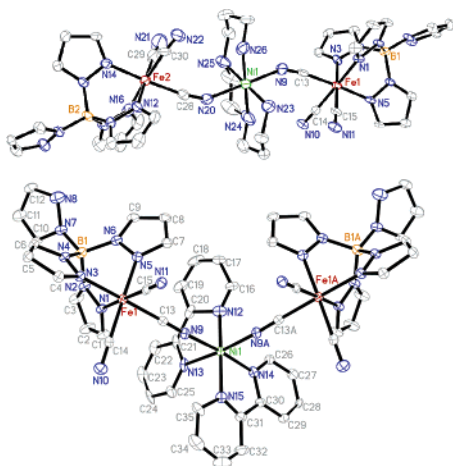


Figure 1. X-ray structure of **2** (top) and one structural isomer of **3** (bottom). Thermal ellipsoids are at the 50% level, and all H atoms and lattice water are eliminated for clarity. Selected bond distances (Å) and angles (deg) for **2**: Fe1–C13, 1.913(8); Fe2–C28, 1.923(8); C28–N20, 1.14(1); Ni1–N9, 2.082(6); Ni1–N20, 2.109(6); Ni1–N9–C13, 150.7(6); Ni1–N20–C28, 149.2(6); N9–Ni1–N20, 179.2(3). For **3**: Fe1–C13, 1.920(5); Ni1–N9, 2.049(4); Ni1–N9–C13, 169.8(4); N9–Ni1–N9A, 90.8(2).

N20) and 2.082(6) (Ni1–N9) Å, while those for the amine range from 2.077(9) (Ni1–N24) to 2.098(9) (Ni1–N25) Å, respectively. The terminal cyanide Fe1–C bond lengths are nearly equivalent [1.933(8) and 1.932(7) Å], with the smallest value [1.913(8) Å] found for the bringing cyanide (Fe1–C13). The terminal Fe–C≡N bond angles range from 174.9(8)° (Fe2–C30–N22) to 177.9(7)° (Fe1–C14–N10), while nonlinear bridging cyanide bond angles [Fe1–C13–N9, 170.4(6)°; Fe2–C28–N20, 170.4(7)°] are found; the Ni–N≡C bond angles are also highly bent, ranging from 149.2(6)° (Ni1–N20–C28) to 150.7(6)° (Ni1–N9–C13), respectively. The intracomplex Fe1⋯Fe2, Fe1⋯Ni1, and Fe2⋯Ni1 contacts are 9.806(2), 4.900(2), and 4.910(2) Å, respectively, while the closest intercomplex contacts between the pyrazole rings and Fe^{III} (Fe1⋯Fe1B) centers are 6.707(2) and 12.881(2) Å, respectively.

Compound **3** crystallizes as a neutral trinuclear complex in the monoclinic $P2_1/m$ space group.^{4,5} The complex consists of a central [Ni^{II}(bipy)₂]²⁺ unit located on a crystallographic mirror plane that is linked to two [(pzTp)Fe(CN)₃][−] anions via *cis*-cyano rather than *trans*-cyano linkages (Figure 1). Symmetry considerations dictate that two structural isomers are found in a 1:1 ratio (Figure S3 in the Supporting Information) for the nonplanar, C_1 -symmetric, trinuclear complex (Figure S4 in the Supporting Information).⁵ The Ni1–N bond distance for the bridging cyanide [Ni1–N9,

2.048(4) Å] is slightly smaller than that in **2**, while those for the coordinated bipy ligands range from 2.02(2) to 2.16(2) Å. For **3**, the terminal cyanide Fe1–C distances are essentially equivalent [1.913(5) and 1.916(5) Å], while a slightly longer bond length [1.920(5) Å] is found for the bridging cyanide (Fe1–C13). The Fe1–C≡N bond angles for the terminal cyanides range from 179.2(4)° to 179.3(4)°, while the bridging cyanide [Fe1–N9–C13, 176.4(4)°] is more acute; the Ni1–N≡C (Ni1–N9–C13) bond angle is 169.8(4)° and is more linear than those in **2**. The intracomplex Fe1⋯Ni1 and Fe1⋯Fe1A contacts are 5.080(1) and 7.747(1) Å, respectively. The closest intercomplex contacts between bipy and pyrazole rings are 3.507(5) Å, while those for the Fe^{III} (Fe1⋯Fe1B) centers are 8.536(1) Å.

The C-bound cyanides are expected to afford low-spin Fe^{III} ($S = 1/2$) centers that exhibit orbital contributions to the magnetic moment and afford g values that deviate significantly from 2.0 (ca. 2.7; see Figure S11 in the Supporting Information).^{2b,3,6–9} The χT vs T data suggest that the Fe^{III} and Ni^{II} ($S = 1$) centers in **2** are ferromagnetically coupled (Figure S5 in the Supporting Information) because the χT product gradually increases from 2.75 cm³ K mol^{−1} (300 K), reaching a maximum value of 3.20 cm³ K mol^{−1} at 5 K; below 5 K, χT decreases toward a minimum value of 2.80 cm³ K mol^{−1} at 1.82 K. On the basis of the trinuclear structure of **2**, the magnetic data have been modeled using an isotropic Heisenberg model in the weak field approximation.⁶ Thus, the theoretical susceptibility has been deduced from the van Vleck equation considering the following Hamiltonian: $H = -2J_1[S_1 \cdot (S_2 + S_3)]$, where J_1 is the isotropic exchange interaction between Fe^{III} and Ni^{II} sites and S_i is the spin operator for each metal center ($S_1 = 1$, Ni^{II}; $S_i = 1/2$, Fe^{III}; with $i = 2$ and 3). When the data below 15 K are neglected to avoid the effects of intercomplex interactions and/or magnetic anisotropy, the best set of parameters obtained is $J_1/k_B = +1.3(1)$ K and $g_{\text{iso}} = 2.50$ (Figure S5 in the Supporting Information).^{5,10} The magnitude of the magnetic exchange through the cyanide bridges is lower than those obtained for other tri- and tetranuclear complexes derived from tricyanoferrate(III) and -nickel(II) centers.^{3,6,7} On the basis of the J_1 value, the first excited state ($S = 1$) is ca. 2.6 K above the $S = 2$ ground state for **2** (Figure S5 in the Supporting Information). Confirmation of this ground state is obtained in the M vs H_{dc} data at 1.85 K because the magnetization is nearly saturated at 7 T, approaching a maximum value of 4.4 μ_B (Figure S6 in the Supporting Information).⁵ ac susceptibility measurements are frequency-independent (Figure S7 in the Supporting Infor-

(4) Crystal data for **1**: C₂₃H₃₂BF₂FeN₁₂, $P2_1/n$, $Z = 4$, $a = 10.2580(2)$ Å, $b = 15.2386(3)$ Å, $c = 16.9913(4)$ Å, $\beta = 96.1396(7)^\circ$, $V = 2640.8(1)$ Å³, $R_1 = 0.0426$, $wR_2 = 0.0851$. Crystal data for **2**: C_{38.5}H₄₈B₂Fe₂N₂₆NiO_{0.5}, $P1$, $Z = 2$, $a = 8.6821(8)$ Å, $b = 16.683(2)$ Å, $c = 18.355(2)$ Å, $\alpha = 76.425(5)^\circ$, $\beta = 76.377(5)^\circ$, $\gamma = 87.918(5)^\circ$, $V = 2511.1(4)$ Å³, $R_1 = 0.0905$, $wR_2 = 0.2453$. Crystal data for **3**: C₅₀H₄₄B₂Fe₂N₂₆NiO₂, $P2_1/m$, $Z = 2$, $a = 8.7275(2)$ Å, $b = 22.6306(6)$ Å, $c = 15.3268(4)$ Å, $\beta = 105.060(1)^\circ$, $V = 2923.2(1)$ Å³, $R_1 = 0.0691$, $wR_2 = 0.0854$. Data were collected at 90.0(2) K on a Nonius Kappa CCD diffractometer (**1**) using Mo K α ($\lambda = 0.71073$ Å) radiation, while **2** and **3** utilized a Bruker Proteum X8 rotating-anode diffractometer with graphite-monochromatized Cu K α ($\lambda = 1.54178$ Å) radiation. Structures were solved by direct methods and refined against all data using SHELXL97.

(5) See the Supporting Information.

(6) (a) Wang, S.; Zuo, J.-L.; Zhou, H.-C.; Song, Y.; You, X.-Z. *Inorg. Chim. Acta* **2005**, 358, 2101–2106. (b) Wang, S.; Zuo, J.-L.; Zhou, H.-C.; Song, Y.; Gao, S.; You, X.-Z. *Eur. J. Inorg. Chem.* **2004**, 3681–3687.

(7) Yang, J. Y.; Shores, M. P.; Sokol, J. J.; Long, J. R. *Inorg. Chem.* **2003**, 42, 1403–1419.

(8) Lescouëzec, R.; Vaissermann, J.; Lloret, F.; Julve, M.; Verdager, M. *Inorg. Chem.* **2002**, 41, 5943–5945.

(9) Kim, J.; Han, S.; Cho, I.-K.; Choi, K. Y.; Heu, M.; Yoon, S.; Suh, B. J. *Polyhedron* **2004**, 23, 1333–1339.

(10) Note that consideration of the intercomplex interactions in the frame of the mean-field approximation did not lead to a better fit of the experimental data.

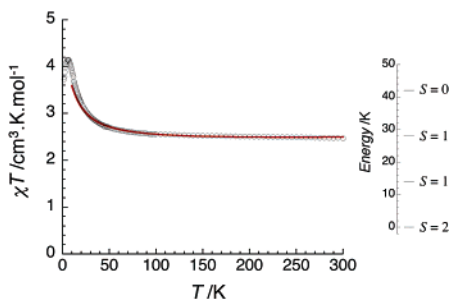


Figure 2. Temperature dependence of χT at 1000 Oe (left) and energy level diagram (right) for **3**. Red line: least-squares fitting of the data.

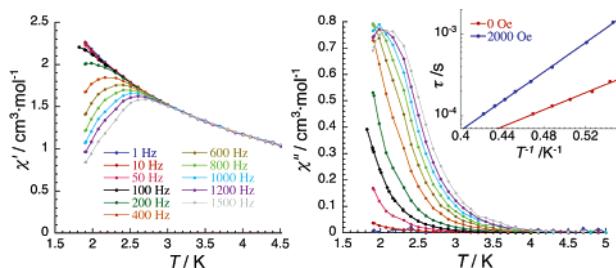


Figure 3. Temperature dependence of the real (χ') and imaginary (χ'') components of the ac susceptibility for **3** ($H_{dc} = 0$ Oe and $H_{ac} = 3$ Oe) between 1 and 1500 Hz. Inset: τ vs T^{-1} plot at $H_{dc} = 0$ and 2000 Oe. The solid lines represent an Arrhenius fit of the data.

mation),⁵ suggesting that **2** is not a SMM in the temperature range measured.

The χT vs T data for **3** suggest that the Fe^{III} and Ni^{II} centers are also ferromagnetically coupled (Figure 2) because the χT product gradually increases from 2.34 cm³ K mol⁻¹ (300 K), reaching a maximum value of 6.01 cm³ K mol⁻¹ at 4 K; below 4 K, χT decreases toward a minimum value of 3.60 cm³ K mol⁻¹ at 1.84 K. Fitting of the magnetic data for **3** gives $J_1/k_B = +7.0(2)$ K and $g_{iso} = 2.31$ (solid line, Figure 2).¹⁰ The magnitude of the magnetic exchange through the cyanide bridges is comparable to those reported for related complexes.^{3,6–9} For **3**, the magnitude of J_1 is much larger than that in **2**, suggesting that the linear cyanide bridges afford more efficient superexchange pathways.^{3,6,7} Scaling with the value of J_1 , the $S = 1$ first excited state for **3** is much higher than that for **2**, being ca. 14 K above the $S = 2$ ground state (Figure 2). Once again the M vs H_{dc} data at 1.85 K support this assumption because the magnetization is nearly saturated, reaching 4 μ_B at 7 T (Figure S8 in the Supporting Information).⁵

The temperature dependence of the ac susceptibility for **3** was measured at several different frequencies at $H_{dc} = 0$ Oe (Figure 3). The ac susceptibility is strongly frequency-dependent, suggesting that **3** exhibits slow relaxation of the magnetization. From the data shown in Figure 3, the relaxation time, τ , can be determined from the maximum of $\chi''(T)$.¹ The relaxation time for **3** follows an Arrhenius law with an energy gap of 12.0 K and $\tau_0 = 4 \times 10^{-7}$ s (inset of Figure 3). As is the case for many SMMs with small spin states,¹¹ it is likely that the observed energy barrier takes an effective value, resulting from a “short-cut” of the thermal barrier by QTM. In zero field, the $\pm m_S$ states have the same energy and QTM between these pairs of levels is possible. When a magnetic field is applied, the $m_S < 0$ and $m_S > 0$

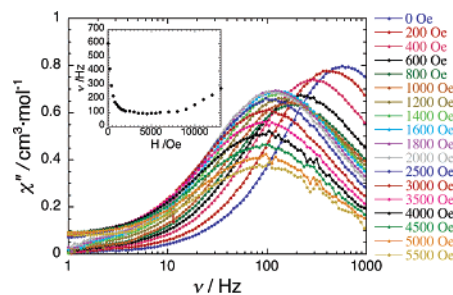


Figure 4. χ'' vs ν plot at 1.85 K under various applied H_{dc} for **3**. Inset: field dependence of the characteristic frequency at 1.85 K.

levels decrease and increase respectively in energy, preventing quantum tunneling between the $\pm m_S$ states.¹

To investigate the activated behavior of **3**, we performed ac susceptibility measurements under several applied dc magnetic fields (Figures 4 and S9 and S10 in the Supporting Information).⁵ At 1.85 K, the characteristic frequency (maximum of the χ'' vs ν plot) decreases rapidly from 600 Hz at 0 Oe and approaches a nearly constant value of 100 Hz between 2000 and 5000 Oe (inset of Figure 4). As shown by this result, the QTM relaxation pathway remains efficient at 1.85 K. τ was thus estimated using the ac data under 2000 Oe (Figure S10 in the Supporting Information). As expected, the relaxation time still follows an Arrhenius law with $\tau_0 = 2 \times 10^{-8}$ s and an energy gap of 20.6 K is found (inset of Figure 3). It is also worth noting that this energy gap allows for an estimation of the uniaxial anisotropy $D/k_B \approx -5.2$ K. Finally, the increase of the characteristic frequency (inset of Figure 4) for fields higher than 5000 Oe is expected because resonant QTM should occur for $H \approx D/g\mu_B \approx 4$ T.¹

In summary, we have described the syntheses, structures, and magnetic properties of two cyanide-bridged trinuclear Fe^{III}₂Ni^{II} ($S = 2$) complexes. Magnetic studies suggest that the magnitude of the magnetic exchange between the Fe^{III} and Ni^{II} centers can be controlled via ancillary ligand choice, and ac susceptibility measurements in a nonzero dc field indicate that **3** is a SMM.

Acknowledgment. S.M.H. gratefully acknowledges the donors of the American Chemical Society Petroleum Research Fund (PRF 38388-G3), the Kentucky Science and Engineering Foundation (Grants KSEF-621-RDE-006 and KSEF-992-RDE-008), and the University of Kentucky Summer Faculty Research Fellow and Major Research Project programs for financial support. R.C. thanks MAGMANet (Grant NMP3-CT-2005-515767), CNRS, Bordeaux 1 University, and the Conseil Régional d'Aquitaine for financial support. G.T.Y. thanks the National Science Foundation (Grant CHE-0210395) for partial financial support.

Supporting Information Available: X-ray crystallographic data in CIF format, experimental details, and additional magnetic data. This material is available free of charge via the Internet at <http://pubs.acs.org>.

IC060379B

(11) For pertinent examples, see: Miyasaka, H.; Clérac, R.; Wernsdorfer, W.; Lecren, L.; Bonhomme, C.; Sugiura, K.-I.; Yamashita, M. *Angew. Chem.* **2004**, *116*, 2861–2865.